

# Comparison of Different Polymeric Multimode Star Couplers for Backplane Optical Interconnect

David Israel, Roel Baets, *Member, IEEE*, Martin J. Goodwin, Nicola Shaw, Mark D. Salik, and Chris J. Groves-Kirkby

**Abstract**—This paper describes a comparison of three types of  $8 \times 8$  multimode star couplers made in polymeric multimode waveguides. Their geometry was designed with a ray tracing tool. Measurements show low loss for all designs, but a symmetrical design, based on a tree of Y-junctions yields the best uniformity.

## I. INTRODUCTION

**O**PTICAL INTERCONNECT is very promising for signal transport in advanced digital systems with high data rates at the board and backplane level. One of the aims of the ESPRIT III project HOLICS (Hierarchical Optical Interconnects for Computer Systems), is the interconnection of  $N$  boards by an optical backplane. In the star coupler topology of Fig. 1, each board can transmit a signal to all  $N$  boards and only one board can transmit at a time. The output from a laser diode on the board is coupled in the backplane, where it is guided to the  $N \times N$  star coupler. This star coupler distributes the light from the input guide to all output guides. The signal in these guides is then detected by a photodiode on each board. Multimode polymeric waveguide boards offer an interesting solution for such interconnect problems because they give the opportunity for a more complex functionality than is possible with point to point links. Also, they allow mass production on large surfaces, the material is flexible and can be used in an acceptable temperature range.

Multimode waveguides have the advantage of relaxed coupling conditions. The large modal volume allows large lateral and/or angular misalignment. Both the size of the laser facet and the divergence angle of the laser beam are small as compared to the waveguide facet and waveguide numerical aperture. Related to the relaxed coupling conditions however is the problem of modal noise. The light coupled from a laser diode will not excite all modes with equal power. There will be a certain modal distribution that strongly depends on the coupling conditions. This uncertainty in modal content effects the performance of multimode waveguide elements (bends, junctions, ...). Therefore, the design of multimode waveguide elements is often more difficult than that of single mode structures.

Manuscript received May 12, 1994. This work was supported in part by the ESPRIT III project 6276 (HOLICS), the Belgian IUAP-24 project, and the GEC-Marconi businesses.

D. Israel and R. Baets are with the Department of Information Technology (INTEC), IMEC-University of Gent, Sint-Pietersnieuwstraat 41, B-9000 Gent, Belgium.

M. J. Goodwin, N. Shaw, M. D. Salik, and C. J. Groves-Kirkby are with the GEC-Marconi Materials Technology, Caswell, Towcester, Northamptonshire NN12 8EQ, U.K.

IEEE Log Number 9411558.

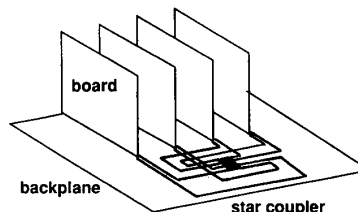


Fig. 1. Boards interconnected with an optical backplane in a star coupler topology.

This paper discusses the design and performance of three realized  $8 \times 8$  star couplers. The structures have been fabricated by DuPont using their Polyguide™ integrated optics system [1]. The waveguides have a rectangular core cross-section. The nominal core area of the guides is  $45 \times 45 \mu\text{m}^2$  (the nominal guide width is  $45 \mu\text{m}$ ). The waveguides are step index guides, the refractive index of the core  $n_{co}$  is 1.53 and 1.5 in the cladding index  $n_{cl}$ . The numerical aperture is 0.3 and the number of modes  $M$  at a wavelength of  $1 \mu\text{m}$ , about 1500 [2].

## II. THE MODELING OF THE STAR COUPLERS

The question arises how to model these highly multimode waveguides. For either single mode or free space problems a lot of algorithms have been developed. For problems where there are only a few modes, one can use theories based on modes. The highly multimodal situation is somewhere in between the single mode case and the free space case, but since we have a quasi continuum of modes it is closer to the free space case where we have a continuum of modes (plane waves).

Techniques where all the modes are traced through the structure are only useful if one can determine the coupling of power between the modes for  $z$ -variant structures as in the coupled mode theory. This will be a difficult task, and even if we could do it, the numerical implementation would ask for large computing times since the number of modes is so large. One can argue to use the beam propagation method (BPM). A disadvantage of this method is that the propagation direction must be the same for all waveguides of the structure. This is no restriction for the star couplers of this paper, but more general structures that appear on the boards cannot be modeled with BPM. Furthermore, BPM requires small propagation steps. This leads to time consuming calculations for structures with a length of several mm to a few cm, as is the case for the multimode polymer waveguide structures.

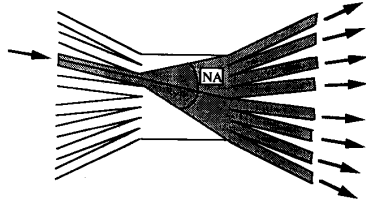


Fig. 2. Short star coupler based on imaging. NA is the numerical aperture of the guides.

We propose to use rays which can be seen as local plane waves. Ray tracing is a widely used technique in free space problems, but also used in waveguide problems [3], [4]. Its major disadvantage is that wave effects as interference and diffraction are neglected. The couplers were modeled with a 3-D ray tracing tool [5], developed specifically for this task. It includes the effects of (polarization dependent) reflection and transmission.

In this ray picture, different modes can be associated with different ray angles [6]. More oblique rays (rays making a larger angle with the guide axis) correspond with higher order modes. A uniform modal distribution corresponds with a uniform distribution of ray angles within the numerical aperture. In this paper, all simulations were done with 2-D ray-tracing. Hereby we excite all possible rays with equal probability in a plane parallel with the substrate. The rays are located in the core, and the ray angles are within the numerical aperture. In [7] we argued that for waveguides with square cross-section this will make only a marginal difference as compared with the 3-D result, where all possible rays are excited within the core and the numerical aperture of the guide, if the structure does not vary in the direction perpendicular to the substrate.

### III. STAR COUPLER DESIGNS

#### A. Introduction

The purpose of an  $N \times N$  star coupler is to couple light from one of its  $N$  input guides to all the  $N$  output guides uniformly (i.e., equal power in all output guides). We assume that the power is uniformly distributed in the excited input, i.e., the power or ray distribution is constant over the waveguide core and is constant within the numerical aperture of the guide.

To obtain very short structures, a star coupler has been designed where the light of the input guide is projected on the array of output guides. The principle of this design is shown in Fig. 2. The guides join the central section such that the light coming from them illuminates all the output guides with approximately the same power. The output guides leave the central section so that the power is coupled efficiently. It is obvious that this design is sensitive to variations in parameters.

Another disadvantage of this design is that the power distribution needs to be perfectly uniform within the numerical aperture to obtain uniform coupling to output guides. However, due to modal noise this is not certain. Since we make use of the large modal volume of multimode waveguides to relax

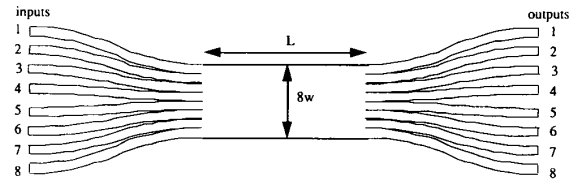


Fig. 3. Mixer rod star coupler.  $L$  and  $8w$  are the length and width of the central mixing section.

the coupling conditions, it is far from evident that all angles within the numerical aperture will be excited equally. A way to cope with this problem is the use of mode scramblers, that randomize ray distributions. However, they add loss to the structure.

It is therefore necessary to look for designs that do not depend so strongly on the modal excitation. If light is coupled in from the input guide to a mixing section where it spreads uniformly over the core of that mixing section, the light can be coupled from the mixing section to all  $N$  output guides. Thus, a uniform distribution of the power over the output guides is obtained. We designed three  $8 \times 8$  star couplers based on that idea, one with a central mixing rod, where combining and splitting is done in a single step, and two based on a tree like structure where the guides are split and combined two by two. These designs are expected to be insensitive to small variations in the parameters. For the modeling we will still assume that the power distributions are uniform.

In all designs we use  $S$ -bends. These are made up of two circular sections with opposite curvature. Earlier work on bends [7] showed that the loss of  $S$ -bends with  $45 \mu\text{m}$  width is acceptable (less than 0.5 dB) for a radius  $R > 16 \text{ mm}$ . The  $S$ -bends used in the designs have therefore  $R > 16 \text{ mm}$ . Furthermore, we found that a uniform power distribution is still uniform after propagation through an  $S$ -bend with  $R > 8 \text{ mm}$ . This is important for guides that join a mixing section with an  $S$ -bend. If the guide is excited with a uniform power distribution, the power distribution will also be uniform when it couples to the mixing section.

#### B. Mixer Rod Star Couplers

In this design, the individual input and output guides join the central mixing section parallel to its axis (see Fig. 3). The offset between the guides is provided by  $S$ -bends with  $R > 16 \text{ mm}$ . The width  $w$  of the input and output guides is  $45 \mu\text{m}$  and the pitch between them  $150 \mu\text{m}$ .

To determine its length  $L$ , the spreading of light in the central mixing section was modeled. Fig. 4 shows the power in the individual outputs 1–8 and the spread of power at the 8 outputs as a function of the mixer length when input 1 is excited uniformly. Losses due to different curvature  $R$  of the  $S$ -bend are neglected in this calculation. The splitting is uniform if  $L$  is larger than a few cm. Fig. 5 gives the results when input 4 is excited uniformly. In this case, the same uniformity is obtained for shorter lengths  $L$ . The results for inputs 2 and 3 can be expected to be in between those for inputs 1 and 4. If we focus on the results for input 1, which

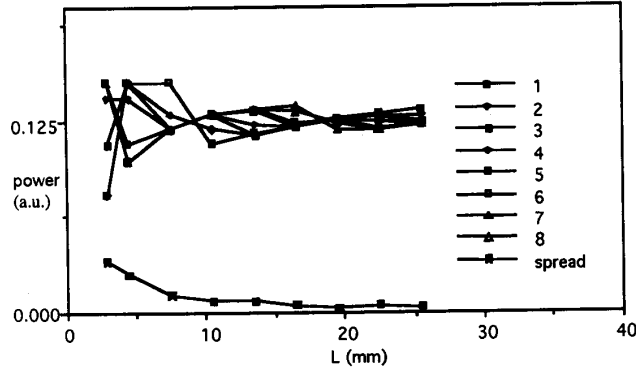


Fig. 4. Simulation of the power in the 8 outputs of the mixer rod star coupler as a function of the mixer length  $L$ . The spread (standard deviation) of the power at the outputs is a measure for the uniformity of the star coupler. Input 1 is excited with a uniform power distribution.

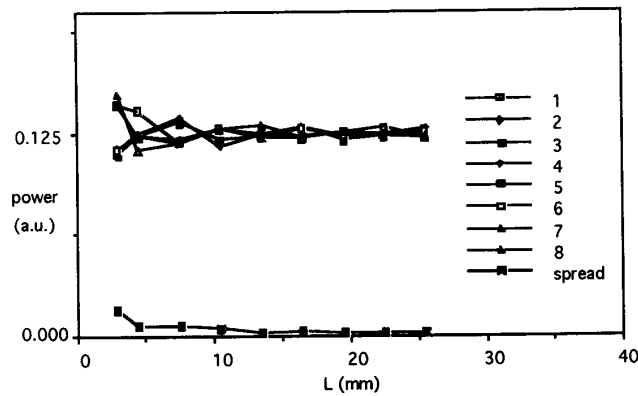


Fig. 5. Simulation of the power in the 8 outputs of the mixer rod star coupler as a function of the mixer length  $L$ . The spread (standard deviation) of the power at the outputs is a measure for the uniformity of the star coupler. Input 4 is excited with a uniform power distribution.

is the worst case, we conclude that the central mixing section must have a length  $L$  larger than 20 mm. This star coupler has been made for  $L = 20, 30,$  and  $40$  mm. The length of the  $S$ -bends is 5 mm. This brings the total length to 30, 40, and 50 mm.

*C. Symmetric Tree Star Coupler*

The different interconnection paths in the mixer rod star coupler have different total bending and as a result different losses. The uniformity of power at the outputs of the coupler will be degraded by this. In the design of Fig. 6, the 8 input guides are combined two by two with symmetrical  $Y$ -junctions to a central mixing section and are split out in the same way. The total bending of all interconnections is equal. The geometry of the junctions and the length of the mixing sections between them, has to be determined so that we have a star coupler with low loss and good uniformity.

Fig. 7 shows three options for the geometry of the  $Y$ -junctions. The waveguide with width  $w$  can be split into two guides with the same width  $w$  (Fig. 7 (a)) or with width  $w/2$  (Fig. 7 (b)). The  $S$ -bends give the junctions a certain pitch. Another possibility is a split to guides with width  $w/2$ , but leaving the main guide under an angle  $\beta$  (see Fig. 7 (c)).

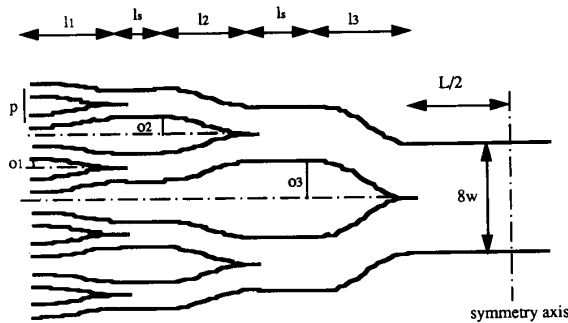


Fig. 6. Symmetric tree star coupler. Only the first half is shown.  $L$  is the length of the central mixing section.  $l_1, l_2,$  and  $l_3$  are the lengths of the  $S$ -bend sections and  $o_1, o_2,$  and  $o_3$  their offset. There are straight guides with length  $l_s$  between the  $Y$ -junctions. The width of the input guides is  $w$  and their pitch  $p$ .

Measurements and modeling results show lower losses for the design of Fig. 7(b) as compared to (a) and (c) if the length and pitch of the splitter are kept constant. Thus, the  $Y$ -junctions used in the design of the symmetric tree star coupler have the geometry of Fig. 7(b). The values used for  $R$  are 16 and 25 mm.

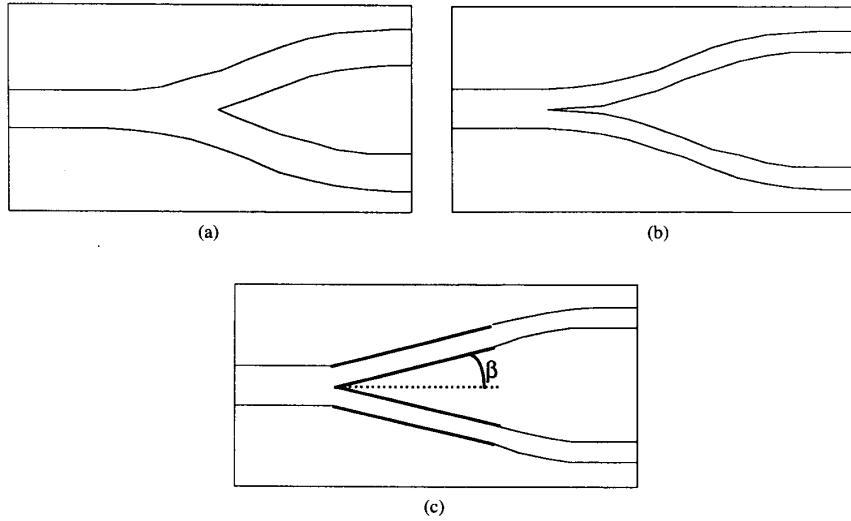


Fig. 7. Three types of Y-junctions, (a) S-bend split to full width arms, (b) S-bend split to half width arms, (c) Angular split.

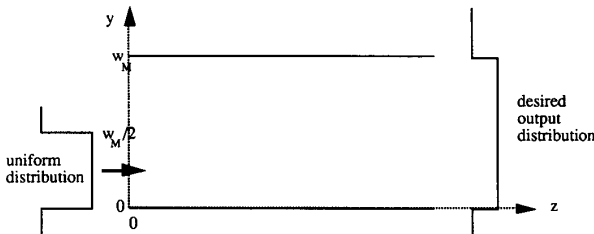


Fig. 8. A mixing section of the tree star couplers. For an appropriate choice of the length  $z$ , a uniform excitation in half of the core will be transformed to a uniform distribution over the entire core.

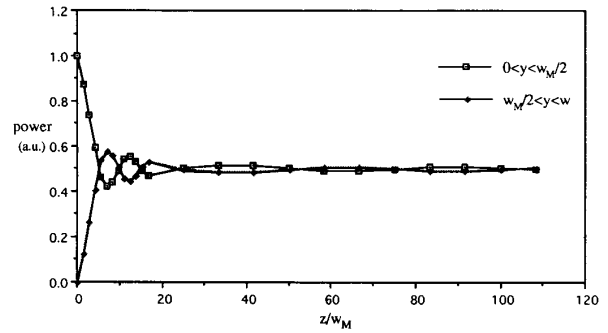


Fig. 9. Simulation of the power in the core of the mixing section (see Fig. 8) versus  $z/w_M$ .

When light is coupled into one of the inputs, the sections (with lengths  $l_2, l_3$  and  $L$ ) of the combining half of the star coupler must randomize a distribution that excites only half of the core with a uniform spatial distribution, to a distribution that fills the core uniformly (see Fig. 8). Since  $R$  is large, we can treat all sections as straight guides. The distribution is considered uniform in a cross-section of the guide with width  $w_M$  if the power in  $0 < y < w_M/2$  equals the power in  $w_M/2 < y < w_M$ . Fig. 9 gives the power in these two parts of the core cross-section as a function of  $z/w_M$ , obtained with the modeling tool.  $z$  scales with  $w$ , due to the geometric scaling of ray paths. For  $z/w_M$  between 10 and 20, the distribution of power is already satisfying. The power is equally distributed if  $z/w_M > 20$ . For  $z/w_M = 20$  we find  $L = 7, 2 \text{ mm} \approx 1 \text{ cm}$  as length of the central mixing section ( $w_M = 360 \mu\text{m}$ ).

The lengths  $l_2$  and  $l_3$  of the other mixing sections have to fulfil  $z/w_M > 20$  as well. For large  $R$ , the length  $l$  of an S-bend with offset  $o$  can be approximated as:

$$l \approx 2\sqrt{o \cdot R}. \tag{3}$$

$l_2$  and  $l_3$  can be found from (3) and Fig. 6:

$$\begin{aligned} o_1 &= \frac{1}{2}(p - w) = \frac{1}{2}(150 - 45) \mu\text{m} = 52.5 \mu\text{m} \\ o_2 &= p - w = 2o_1 \\ o_3 &= 2(p - w) = 4o_1 \end{aligned} \tag{4}$$

$$\begin{aligned} l_1 &\approx 2\sqrt{o_1 \cdot R} \\ l_2 &\approx 2\sqrt{o_2 \cdot R} = \sqrt{2}l_1 \\ l_3 &\approx 2\sqrt{o_3 \cdot R} = 2l_1. \end{aligned} \tag{5}$$

For  $R = 16 \text{ mm}$  we find  $l_2 = 2.6 \text{ mm}$  and  $l_3 = 3.7 \text{ mm}$ . This leads to the values 29 and 20 for  $z/w_M$  respectively. Thus  $z/w_M > 20$  for all mixing sections. If  $R = 25 \text{ mm}$ , the uniformity will improve.

To further improve the uniformity, straight guides with length  $l_s = 2 \text{ mm}$  are added between the S-bends and the Y-junctions. The total length of the star coupler is 38 mm for  $R = 16 \text{ mm}$  and 42 mm for  $R = 25 \text{ mm}$ .

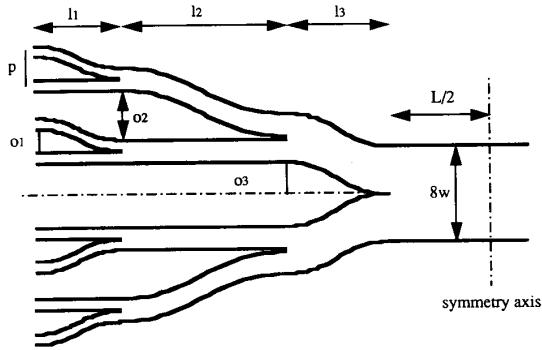


Fig. 10. Asymmetric tree star coupler. Only the first half is shown.  $L$  is the length of the central mixing section.  $l_1$ ,  $l_2$ , and  $l_3$  are the lengths of the  $S$ -bend sections and  $o_1$ ,  $o_2$ , and  $o_3$  their offset. The width of the input guides is  $w$  and their pitch  $p$ .

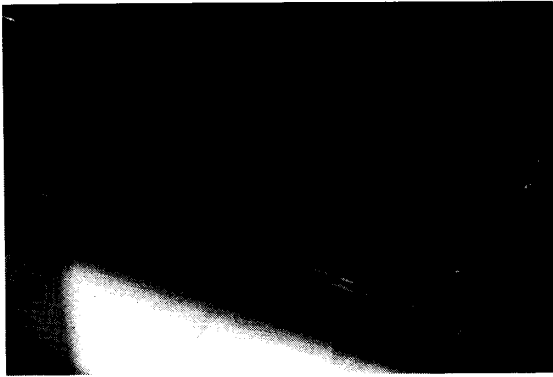


Fig. 11. Photograph of the polymer waveguide sample, containing the realized structures. The size of the sample is 70 mm  $\times$  25 mm.

#### D. Asymmetric Tree Star Coupler

The lengths of both the mixer rod and the symmetric tree star couplers are rather long. Shorter structures can be obtained with the asymmetric design of Fig. 10. The number of  $S$ -bends is minimized and the straight sections between  $S$ -bends and  $Y$ -junctions are left out. The  $Y$ -junctions split the guides to half the width, but they are asymmetrical, only one of the branches is an  $S$ -bend. The values used for  $R$  (radius of the bent sections) are 16 and 25 mm, and for the central section we take  $L = 1$  cm, as with the symmetrical tree.

The lengths  $l_2$  and  $l_3$  of the other mixing sections can be found from Fig. 10 and (3):

$$\begin{aligned} o_1 &= p - w = (150 - 45) \mu\text{m} = 105 \mu\text{m} \\ o_2 &= 2(p - w) = 2o_1 \\ o_3 &= \frac{1}{2}(p - w) = 2o_1 \\ l_1 &\approx 2\sqrt{o_1 \cdot R} \\ l_2 &\approx 2\sqrt{o_2 \cdot R} = \sqrt{2}l_1 \\ l_3 &\approx 2\sqrt{o_3 \cdot R} = \frac{1}{\sqrt{2}}l_1. \end{aligned} \quad (6)$$

(7)

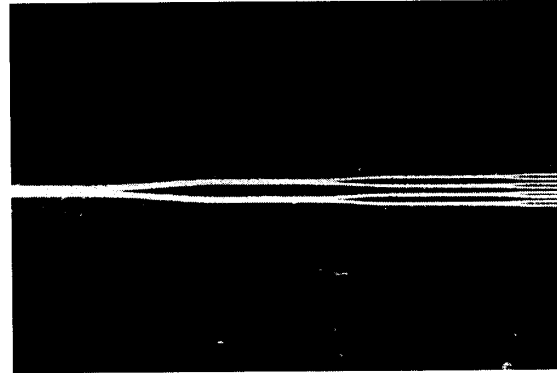


Fig. 12. This photograph shows the splitting section of the symmetric tree star coupler ( $R = 25$  mm) when He-Ne laser light is coupled into input 1.

For  $R = 16$  mm we find  $l_2 \approx 3.7$  mm and  $l_3 \approx 1.8$  mm. This leads to the values 41 and 10 for  $z/w$  respectively. The value  $z/w = 10$  for  $l_3$  is rather low, but Fig. 9 shows that the distribution of power is already acceptable about that point. The situation improves for  $R = 25$  mm there we find  $z/w$  values 51 and 13 for  $l_2$  and  $l_3$  respectively. Thus, the lengths  $l_2$  and  $l_3$  of the mixing sections are long enough. The total length of the asymmetric tree star coupler is 26 mm for  $R = 16$  mm and 30 mm for  $R = 25$  mm. These designs are about 30% smaller than the symmetrical designs, for the same value of  $R$ .

#### IV. EXPERIMENTAL RESULTS

All structures designed in Section III were realized with the polymer waveguide technology Polyguide<sup>TM</sup> of DuPont [1]. The polymer waveguide sample with the realized structures on is shown in Fig. 11. Fig. 12 is a photograph of the splitting part of the symmetric tree star coupler ( $R = 25$  mm) when light from a He-Ne laser is coupled into input 1. The splitting to the 8 output guides can be seen clearly.

Measurements were done to determine the losses and uniformity of the realized structures. We transformed the beam of a YLF laser at  $1.047 \mu\text{m}$  to a point source with  $NA = 0.35$ . This is the best match with the numerical aperture of the waveguide. For the mixer rod star couplers and the symmetric tree star couplers, we coupled this point source at inputs 1, 4, and 6 (the inputs are numbered as in Fig. 3). In the asymmetric tree structures we coupled in at all 8 inputs. The power at all 8 outputs has been measured for each excitation. When a uniform point source is coupled in a multimode step index waveguide, the light will after soon spread to a uniform power distribution over the core and within the numerical aperture. This is analogous to the mixing in the mixer rod star coupler. For guides with a width of  $45 \mu\text{m}$ , the power is uniform after a length of a few mm. The length of the guides on the sample, before they combine in the star coupler, is several cm. Therefore, a uniform power distribution will be coupled in the star couplers when the input guides are excited with the uniform point source.

TABLE I  
SUMMARY OF RESULTS FOR THE STAR COUPLERS

TYPE	parameters	total length (mm)	max. excess loss (dB)	average excess loss (dB)	uniformity (dB)
mixer rod	L=2 cm	30	-2.43	-0.24	1.37
mixer rod	L=3 cm	40	-3.65	-0.71	1.48
mixer rod	L=4 cm	50	-2.57	-0.34	1.42
symm. tree	R=16 mm	38	-2.36	-1.73	0.54
symm. tree	R=25 mm	42	-0.80	-0.16	0.40
asymm. tree	R=16 mm	26	-4.13	-1.57	1.23
asymm. tree	R=25 mm	30	-2.64	-0.70	0.97

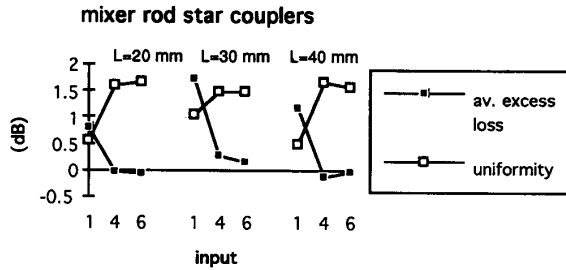


Fig. 13. Average excess loss and uniformity (standard deviation) of the outputs for inputs 1, 4, and 6 of the mixer rod star couplers.

The total loss in an interconnection path (one input to one output) consists of several parts:

$$\begin{aligned} \text{total loss} = & \text{straight guide loss} \\ & + \text{splitting loss} + \text{excess loss.} \end{aligned} \quad (8)$$

The straight guide loss includes absorption and scattering loss and is 0.35 dB/cm. The splitting loss to 1/8 of the power is fundamental and equals 9.03 dB. The excess loss depends on the geometry of the structure. It includes all losses due to the deviation of the structure from a straight guide, e.g., bending losses. In what follows we shall discuss the excess loss of the interconnection paths of the different star couplers.

#### A. Summary of Results

Table I shows the statistics over all measured interconnection paths (links) for each star coupler. The number of measured links is 24 for all structures (inputs 1, 4 and 6 to all outputs) except for the asymmetric tree structures, there we measured all 64 links. The standard deviation of the excess loss of the links is a measure for the uniformity of the output power of the devices. A small standard deviation or uniformity indicates that the splitter is uniform. This uniformity is also shown in the table.

Table I shows that the uniformity of the mixer rod devices is poor although the loss is low. The performance of this star does not improve for longer lengths  $L$  of the central mixing section. The tree structures have a better uniformity. The symmetric star, with extra long mixing lengths yields the best results. We will now discuss the measurements in more detail.

#### B. The Mixer Rod Star Coupler

Fig. 13 shows the average excess loss and uniformity over the 8 outputs for inputs 1, 4, and 6 of the mixer rod star couplers. The average excess loss depends on the input. The inner  $S$ -bends, that join the central mixing section close to

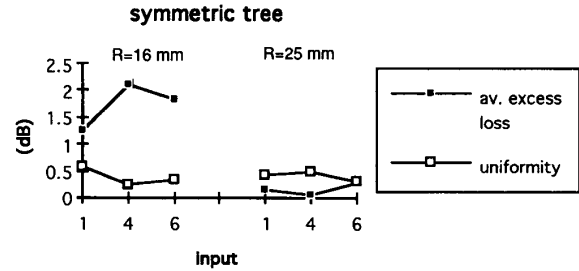


Fig. 14. Average excess loss and uniformity (standard deviation) of the outputs for inputs 1, 4, and 6 of the symmetric tree star couplers.

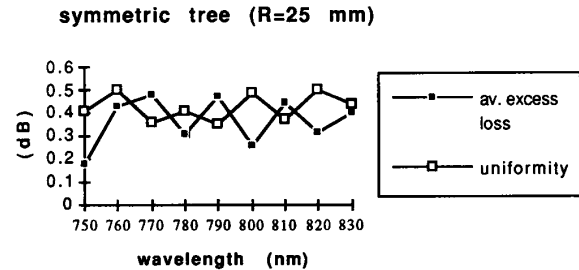


Fig. 15. Average excess loss and uniformity (standard deviation) of the outputs for input 1 of the symmetric tree star coupler ( $R = 25$  mm) as a function of wavelength.

its axis, have smaller losses due to their larger radius  $R$ . The uniformity of these structures is not so good, due to the different  $S$ -bend losses.

#### C. The Symmetric and Asymmetric Tree Star Couplers

The average excess loss and uniformity for 3 inputs of the symmetric tree star coupler is shown in Fig. 14. Low loss is measured for  $R = 25$  mm. The uniformity is about 0.5 dB. Less than 0.5 dB is a good target for the uniformity of a star coupler, and we are near this target.

A collimated beam ( $NA = 0.05$ ) from a tuneable Ti-Sa laser was coupled into input 1 of the symmetric tree. For different wavelengths, different modal distributions are excited. Fig. 15 shows the average excess loss and uniformity for all outputs versus wavelength. The uniformity is again about 0.5 dB and the loss corresponds with the values of Fig. 14. This measurement indicates also that the performance of this coupler does not depend much on the NA of the input beam.

The average excess loss and uniformity for all 8 inputs of the asymmetric tree star coupler is shown in Figs. 16 and 17. The uniformity is about 1 dB in both cases. The loss is below 1.5 dB for  $R = 25$  mm.

#### D. Variations Due to Different Coupling Conditions

We measured variations due to different coupling conditions for the tree star couplers. The spot of the point source was moved to 9 different locations on the input facet. Fig. 18 shows the average excess loss and uniformity for (statistics over the 9 input locations) for all outputs and one input. The uniformity is about 0.5 dB for the symmetric tree (excitation

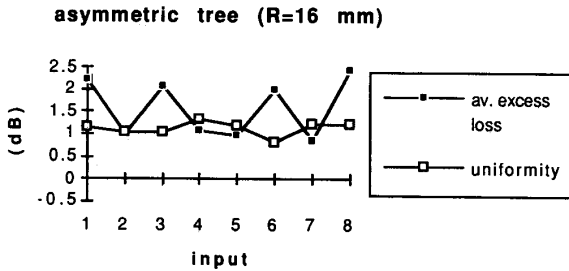


Fig. 16. Average excess loss and uniformity (standard deviation) of the outputs for all inputs of the asymmetric tree star coupler ( $R = 16$  mm).

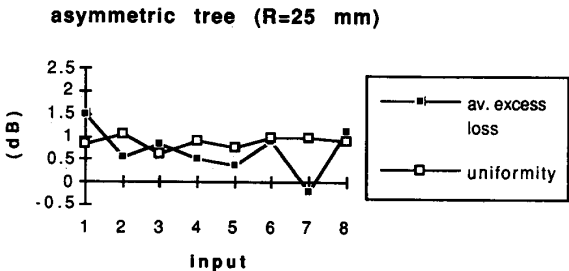


Fig. 17. Average excess loss and uniformity (standard deviation) of the outputs for all inputs of the asymmetric tree star coupler ( $R = 25$  mm).

in input 1) and is only slightly larger for the asymmetric tree (excitation in inputs 1 and 4). Different coupling conditions excite different sets of modes. The value 0.5 dB is a measure for the fluctuations due to modal noise.

## V. DISCUSSION

Table I and Fig. 13 show that the measured performances of the mixer rod type do not depend on the length  $L$  of the mixing section. There is no trend that loss or uniformity improves for larger  $L$ . On the contrary, the performance is best for the shortest  $L$ . We conclude that the mixing is already optimal for  $L = 2$  cm, as was predicted with the ray-tracing tool. The bad uniformity is probably due to the different losses of the  $S$ -bends, leading to different output power if the splitting was uniform.

The uniformity of the symmetric tree (see Table I and Fig. 14) is only slightly improved if  $R$  is changed from 16 to 25 mm. This again indicates that the mixing lengths are sufficiently long. The losses depend on  $R$ , with very low loss for  $R = 25$  mm. Fig. 14 shows that there is no dependence of the loss and uniformity on the input, as was expected from the symmetry.

The symmetric tree has a uniformity that is twice as good as the uniformity of the asymmetric tree. This indicates that mixing lengths in the asymmetric tree have been chosen too short. Due to the asymmetry, the average excess loss depends on the input (see Figs. 16 and 17).

In the designs of the symmetric and the asymmetric tree, the same radius  $R$  has been used for all bent sections. However, we found that the loss of a circular bend is a function of  $w/R$  [7]. The same dependence on  $w/R$  is expected for  $S$ -bends.

## uniformity for different excitations

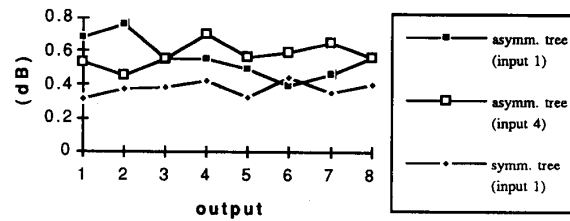


Fig. 18. Uniformity of the tree star couplers for different excitations with a point source.

Thus, if the  $S$ -bends in the tree-like designs have the same value for  $w/R$ , they will have the same loss. The losses will be distributed equally over all  $S$ -bends. For future designs we propose to take the same  $w/R$  for all  $S$ -bends.

## VI. CONCLUSION

We designed 3 different types of  $8 \times 8$  star couplers for various parameters, resulting in 7 designs. Two of the three types are based on trees of  $Y$ -branches, the third one on combining the 8 guides with  $S$ -bends to a central mixing section. In each of the designs the length of the waveguide sections in between the junctions was chosen such that the ray distribution was uniform.

Experimental results at  $1.047 \mu\text{m}$  show low loss for all structures. The excess loss of the structures is mainly determined by the radius  $R$  of the bent sections. The uniformity of power at the output waveguides is best for the symmetric tree structure and is about 0.5 dB. Measurements with a tuneable Ti-Sa laser show that the loss and uniformity is independent of the wavelength in the range 750–830 nm. Furthermore, the loss and uniformity were found to be insensitive of changes in the coupling conditions of the focused laser beam onto input guides. This confirms again that the central mixing sections of the star couplers were well designed.

## ACKNOWLEDGMENT

The authors acknowledge the Du Pont Polyguide™ team (B. L. Booth, J. E. Marchegiano, C. T. Chang *et al.*) for the fabrication of polymer waveguide samples.

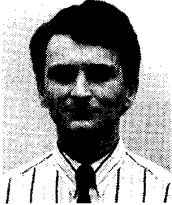
## REFERENCES

- [1] B. L. Booth, "Polymers for integrated optical waveguides," in *Polymers for Electronic and Photonic Applications*, C. P. Wong, Ed. Boston, MA: Academic Press, Harcourt Brace Jovanovich, 1992, pp. 549–597.
- [2] C. P. Pask, A. W. Snyder, and D. J. Mitchell, "Number of modes on optical waveguides," *J. Opt. Soc. Am.*, vol. 65, p. 356, 1975.
- [3] R. G. Hunsperger, *Integrated Optics: Theory and Technology*. Berlin: Springer-Verlag, 1985, pp. 24–29.
- [4] A. W. Snyder and J. D. Love, *Optical Waveguide Theory, Part I*. London: Chapman and Hall, 1983.
- [5] D. Israel and R. Baets, "Analysis of multimode polymeric waveguide structures," in *Abstracts SIOE '93, UWCC*, Cardiff, Wales, 1993.
- [6] Y. Kokubun, S. Suzuki, and K. Iga, "Phase space evaluation of distributed-index branching waveguides," *J. Lightwave Technol.*, vol. LT-4, pp. 1534–1541, 1986.
- [7] D. Israel, R. Baets, N. Shaw, and M. Goodwin, "Study of multimode polymeric waveguide bends for backplane optical interconnect," in *Tech. Dig. MOC/GRIN '93*, Kawasaki, Japan, 1993.



**David Israel** received the degree in electrical engineering (specialization in physics) from the University of Gent, Belgium, in 1991.

Since then he has been with the Department of Information Technology (INTEC) of the University of Gent, where he works towards the Ph.D. degree. His research includes the modeling and characterization of polymer multimode waveguides for passive optical interconnections, work that is done within the ESPRIT "HOLICS" project.



**Roel Baets** (M'88) received the degree in electrical engineering from the University of Gent, Belgium, in 1980. He received the M.Sc. degree in electrical engineering from Stanford University in 1981 and the Ph.D. degree from the University of Gent in 1984.

Since 1981 he has been with the Department of Information Technology (INTEC) of the University of Gent. Since 1989 he has been a professor in the engineering faculty of the University of Gent. Since 1990 he has also been a part-time professor at the Technical University of Delft, The Netherlands. He has worked in the field of III-V devices for optoelectronic systems. With over 100 publications and conference papers he has made contributions to the modeling of semiconductor laser diodes, passive guided wave devices and to the design and fabrication of OEIC's. His main interests now are modeling, design and testing of optoelectronic devices, circuits and systems for optical communication and optical interconnect.

Dr. Baets is a member of the Optical Society of America, SPIE and the Flemish Engineers Association. In 1994 he served as a member of the program committee of ECOC and of the IEEE International Laser Conference.

**Martin J. Goodwin** received the degree of B.A. (Honours) in physics in 1981 from Oxford University, and joined the Optics Group at GEC-Marconi Materials Technology (then Plessey Research Caswell) later that year to work on integrated optics in Lithium Niobate. Since then he has worked on nonlinear integrated optics, organic electro-optic polymers, optical computing and interconnects, and electro-optic probing of MMIC's. He has published over 50 papers and conference presentations in these areas. He is now responsible for coordinating GMMT's work on optical sensors, passive optical devices and optical interconnect technologies. He was responsible for GEC-Marconi's work within the ESPRIT "OLIVES" project on optical interconnection of VLSI circuits, and is now Project Manager for the ESPRIT "HOLICS" project on hierarchical optical interconnection systems.

Mr. Goodwin is a member of the Optical Society of America.

**Nicola Shaw** (nee Wilson) graduated from Cambridge University with the B.A. degree in natural sciences (physics) in 1988.

Since then she has worked for GEC-Marconi Materials Technology (formerly Plessey Research and Technology). Initially her work in the integrated optics group focused on the development of waveguide devices in III-V semiconductors for signal processing in telecommunications. This involved the development of technologies for monolithic integration of optical and electronic functions in InP within RACE (OSCAR). More recently she has been involved in the research of passive optical interconnects, e.g., under ESPRIT (HOLICS), and GaAs based waveguide devices.

**Mark D. Salik** graduated from Birmingham University in 1988 with a degree in physics. He joined the University of Alberta, Canada, as a teaching assistant and completed a Master's degree in solid state physics in 1990, with research on the photoluminescence of GaAs.

He joined GEC-Marconi Materials Technology in 1991 and worked on laser FM response measurements, coherent communications systems and polymer waveguide characterization.

**Chris J. Groves-Kirkby** received the B.Sc. degree in applied physics from the University of Durham in 1964 and the Ph.D. degree from the same University in 1967 for his thesis entitled "EPR Linewidths in Maser Materials."

From 1967-1969 he was a Departmental Research Officer in the Clarendon Laboratory, University of Oxford, studying optical spectroscopy of rare-earth salts. He joined the former Plessey Company (now part of GEC-Marconi) in September 1969, to work on applications of transparent ferroelectric ceramic materials to displays; he has been active in developing a number of further applications for these materials, principally as laser Q-switches, page compositors for holographic storage systems, high-speed shutters for flash protection and, most recently, as spatial light modulator array devices for digital optical computing and optical interconnection. Study of the applications of organic photochromic materials as spatial light modulators led to the development and construction of a Fourier transform processor for nonoptical holographic data and, more recently, the demonstration of optical bistability in the same materials. In integrated optics, he was involved in early guided-wave modulator development at Caswell and he has contributed to the ongoing research on semiconductor waveguide modulators; in addition, he has been responsible for the development of acousto-optic SAW Bragg cells for acousto-optic signal processing and the construction and delivery of prototype acousto-optic spectrum analyzer systems. Activities in the area of fiber optics include the development of components for all-optical frequency- and time-domain signal processing, together with the design and construction of all-fiber band-pass filter and code-generator systems. In the area of optical interconnection, he was responsible for the high-frequency characterization of MQW modulator arrays, establishing a free-space optical interconnect demonstrator incorporating these devices. He currently manages a multiestablishment collaboration in the area of optical backplane technology. He is the author of more than 50 technical papers and conference presentations and has been responsible for 11 patent applications covering diverse aspects of optical data processing.

Dr. Groves-Kirkby is a Member of the Institute of Physics (London).